



Tree root-soil interaction: field study of the effect of trees on soil moisture and ground movement in an urban environment

Xi Sun · Jie Li

Received: 19 March 2023 / Accepted: 21 September 2023
© The Author(s) 2023

Abstract

Aims Little research has been conducted to quantify the atmosphere-plant-soil interaction in urban environments due to a lack of understanding of plant water use characteristics and the limited availability of high-quality field data. This research aims to quantify the drying effect of root systems of two Australian native tree species on soil water dynamics and ground movement using high-quality field measurement data.

Methods A long-term field monitoring on soil moisture variation and ground movement close to *C. maculata* and *M. styphelioides*, was conducted for up to 45 months in Melbourne, Australia. The water requirement of each tree was monitored using sap flow sensors. Laboratory soil testing was conducted to obtain soil properties and develop profiles of soil suction and water content. The intercorrelation between soil water dynamics and tree soil water use was established.

Results Tree roots could no longer extract water from the soil when total soil suction exceeded a wilting point of approximately 1000 kPa. The soil profile

differences between the two sites were a significant factor causing substantial differences in tree water consumption.

Conclusions At the *C. maculata* site, tree-induced soil desiccation occurred to a depth of 1.1 m, while at the *M. styphelioides* site, it extended down to 2.2 m depth. The tree root-soil interaction analysis shows that water uptake of 10.64 kL by tree roots partially contributes to a 5% decline in soil water content and a 270 kPa rise in soil suction, resulting in a continuous soil settlement of 22 mm.

Keywords Expansive soil · Plant-soil interaction · Sap flow · Soil movement · Soil suction · Tree water uptake

Introduction

Expansive clay soils undergo significant volume changes in response to changes in moisture, expanding during wet seasons and contracting during dry ones. Trees growing near residential houses can extract a substantial amount of water from the soil, particularly during dry seasons, leading to differential movement in the foundation soils. This differential movement can cause severe damage to the footing and building. In Victoria, Australia, Holland (1981) reported that almost all foundation failure cases in Quaternary basaltic clays were due to the drying settlement of expansive soils beneath the building, while

Responsible Editor: Oscar Pérez-Priego.

X. Sun · J. Li (✉)
School of Engineering, RMIT University, Melbourne,
VIC 3001, Australia
e-mail: jie.li@rmit.edu.au

X. Sun
e-mail: xi.sun@rmit.edu.au

three-quarters of failures in Tertiary to Ordovician clays were caused by local drying settlement resulting from closer distances between plants and dwellings.

Trees need to expand their feeder root at a greater distance to search for water during dry months, while unrestricted water access could result in a smaller root system. Ng et al. (2020) found that the capacity of trees to absorb water remained at the highest level before reaching the wilting point soil suction threshold. Mature tree roots are typically developed 1–2 m below the ground surface, with the greatest density of roots within the top half meter, while the lateral roots may extend more than 10 m from the tree trunk (Dobson and Moffat 1995). Cameron (2001) demonstrated that the desiccating effects of a single tree could reach up to 5 m deep during dry months, and this depth could increase to 6 m for a group of trees. Li and Guo (2017) concluded that the influence depth of a 15 m tall Eucalypt tree was approximately 3.5 m. Through the study of soil moisture in the vicinity of poplar trees, Biddle (1983) found that the lateral impact of tree roots can extend as far as the height of the tree. However, the tree's influential distance and depth suggested by these studies were primarily based on soil suction/moisture tests conducted once or twice during site investigation or short-term site monitoring, which could lead to underestimation of the tree's effects on soil.

Soil, plants, and the atmosphere are interconnected through complex physical and biological interactions. A better understanding of the significance of the soil water balance, which is controlled by the soil, plants and atmosphere, on plant water usage could be obtained from modeling soil water dynamics (Verma et al. 2011). Given that the mechanism by which plants absorb water is controlled by the differential in water potential between the soil and roots (Dasgupta et al. 2015), the boundaries of soil water potential can be utilized to quantitatively assess the relationships between plants and soil.

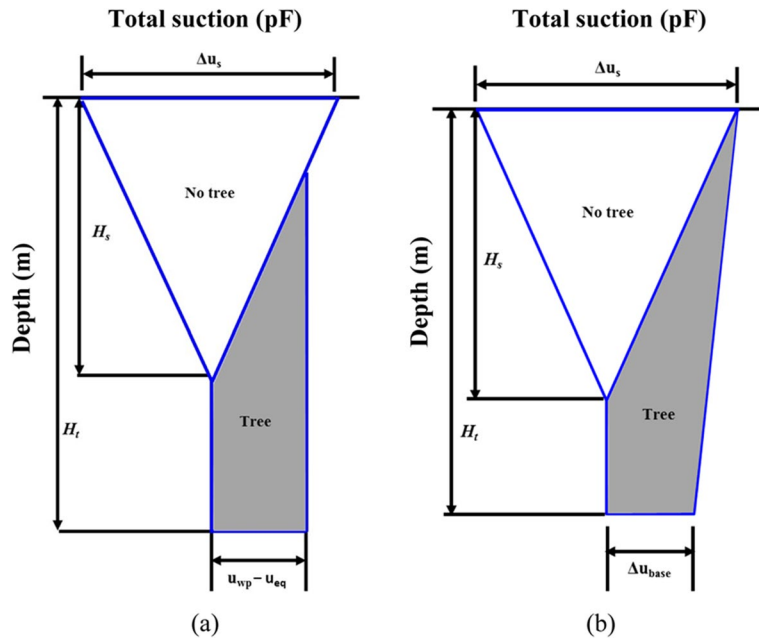
Various models have been developed to simulate the movement of water from soil to the atmosphere based on the hypothesis of cohesion-tension (Couvreur et al. 2018). Teodosio et al. (2017) proposed a porous-media model that integrates the continuity equation with Darcy's law to simulate soil-plant root interaction. Manoli et al. (2014) established a 3D plant–soil model based on Richard's Equation to examine the impact of the roots of pine trees on

soil water dynamics. Silva et al. (2022) developed a FETCH3 model to estimate the water flows via the soil-plant-atmosphere continuum (SPAC).

The Australian Standard AS2870 (2011) provided an extra design soil suction change and an additional depth to cope with the influence of trees on the design of residential footing. The “normal” design soil suction change caused by local climate together with the suction change due to the tree root drying effect are presented in Fig. 1. H_s represents the depth below which the soil suction remains unaffected by climate variations, while H_t signifies the maximum drying depth induced by trees. The “normal” design suction change without the effect of the tree was assumed to be symmetrical for all climatic regions (e.g. equal wetting and drying over the life of the building). The shaded areas of suction change due to the tree effect are equivalent between the wilting point approach (Fig. 1a) and the design compromise (Fig. 1b). Conservative values of the additional tree-induced suction change Δu_{base} are given in AS2870 (2011) for design purposes. However, these empirical values were based on the limited number of case studies, adding risks of footing failure due to inappropriate design. Besides, information such as water demand and tree species were not considered at the time of revising the guidelines. This study validated these empirical values outlined in the Australian building standard by developing soil suction profiles for the two experimental sites using long-term, in-situ soil suction datasets. Long-term soil water usage information for two popular Australian native tree species was also provided.

This study was based on the hypothesis that soil water uptake by different tree species induces measurable desiccation effects in surrounding soils, which can be characterized through in-situ field measurements of sap flow, soil moisture and suction, and soil movement. Throughout this research, soil hydrologic properties and soil movement in close proximity to the studied trees were closely monitored for a duration of up to 45 months. The primary goal of this research was to investigate the drying effect of root systems of two tree species by establishing the intercorrelation between tree soil water use and soil water dynamics, as well as ground surface movement using high-quality field datasets.

Fig. 1 Design suction change profile **a** theoretical **b** equivalent suction change distribution



Materials and methods

Experimental field sites

Two individual Australian native tree species, *Corymbia maculata* (Hook) K.D Hill & L.A.S Johnson and *Melaleuca styphelioides* Sm., grown in two well-instrumented experimental sites (37°51'S, 145°16'E; 37°52'S, 145°17'E) in the southeast suburb of Melbourne, Australia, were selected for monitoring soil movements at the ground surface and sub-ground, soil moisture and tree sap flow rate.

The location of various monitoring instruments relative to the tree is depicted in Fig. 2. The chosen species have been widely planted in parks, reserves and road verges in the southeast region of Australia. All sites have an altitude of 80 m and are located in Climatic Zoning 3 (Li and Sun 2015; Sun et al. 2017). Based on a 60-year climatic record (1960–2020), the mean yearly temperature and precipitation are 14.8 °C and 828.7 mm, respectively (BOM 2022). The mean yearly solar exposure is 14.8 MJ m⁻². Each tree was installed with a sap flow sensor, secured by a cage consisting of six steel wire mesh panels. A shade sheet was installed on the cage to prevent strong sunlight. Two 12 V batteries placed in a protective box were used to recharge the sap flow instrument. Tree heights of 14.5 m and 8.6 m and crown diameters of

11.9 m and 7.5 m were measured for *C. maculata* and *M. styphelioides*, respectively. Both trees are more than 50 years old.

Field site instrumentation

A number of monitoring instruments, including in-situ soil hygrometers, soil movement probes, Neutron Moisture Meter (NMM) access tubes and Sap Flow Meters (SFM1), were installed at the *C. maculata* and *M. styphelioides* sites in spring 2017. Details for the instruments employed are described in the following sections.

Soil suction

To obtain total soil suction in the vicinity of the monitored trees, a number of in-situ soil hygrometers (Wescor PST-55) were installed at various depths in the pre-drilled borehole located close to the tree's dripline. A 0.15 m diameter PVC pipe was cut to a length of 0.3 m and was installed at the top of the borehole and closed with a cast iron cover. The surface was finished with a 10% slope to drain water away from the cover. While reading was taken, the thermocouple junction was cooled below the dew point of air surrounding the soil by a cooling current, leading to water condensing on the junction. A

◀ **Fig. 2** The layout of the two experimental sites (not to scale) **a** *C. maculata* site **b** *M. styphelioides* site

voltage is generated through equilibration between water evaporation and condensation, which is then converted to total suction. The sodium chloride solution at various concentrations were prepared to calibrate each hygrometer prior to installation. The water potential system PSYPRO, with an accuracy of 0.01–0.1 MPa, was employed to record in-situ soil suction reading at various depths. The PSYPRO Manual suggests that suction values below the lower limit of 50 kPa should be considered with caution.

The design soil suction change profile (Fig. 1) will be established against the soil suction profile developed based on the field measurements by hygrometers for the two study sites. AS2870 (2011) specified that the maximum surface design suction change value is 1.2 pF, equivalent to 1.2 log (kPa). An assumption was made that the design suction change decreased linearly with depth and no climate-induced soil suction change occurred below the depth of design suction change H_s . The additional suction change caused by trees can be determined using values of the wilting point soil suction u_{wp} and the deep equilibrium soil suction u_{eq} obtained from field site measurements. u_{wp} is the soil suction beyond the threshold above which tree roots are not able to absorb water from soils, while u_{eq} is the soil suction that would not vary due to climatic changes.

Soil movement

A number of ground surface movement pads and sub-surface probes were installed at different distances from the monitored trees to evaluate the effect of tree drying on soil movement. The surface movement pad comprised a 11 cm long, 2.5 cm diameter steel rod attached to a cylinder concrete pad (10 cm high × 10 cm diameter), while the sub-surface probe comprised a 2.5 cm diameter steel rod with a length from 0.5 to 1 m fixed to a 5 cm high and 8 cm diameter cylinder concrete block. At the field sites, boreholes (BHs) were drilled to depths of 0.5 and 1.0 m and sleeved with PVC pipes allowing sub-surface probes to be installed at the bottom of BHs. The top end of the PVC pipe was closed with a locking cap preventing the ingress of rainwater and debris.

A row of five galvanized steel survey pins spaced at 1 m was installed on the asphalt footpath, located 10 m south of the *C. maculata*. Three surface pads were installed at 7 m (pad 1), 11 m (pad 2) and 14.5 m (pad 3), respectively, from the tree, whereas the 0.5 and 1.0 m sub-surface probes were installed at 7.5 and 8.5 m away from the tree (Fig. 2a). These monitoring points were located on the west side of the tree. A row of four surface pads spaced at 2 m was installed at 4.0 m, 6.0 m, 8.0 m and 10.0 m, respectively, from the *M. styphelioides*, while the 1.0 m sub-surface probe was located at 6.3 m distant from the tree (Fig. 2b). Movements of surface and sub-surface soil were measured using a laser level. The levels of soil were compared to the reduced level of the benchmark constructed in close proximity. The original level obtained in the spring of 2017 was used to determine soil movements. Positive soil movements imply heave, whereas negative movements suggest a settlement. Level surveys were conducted from Oct 2017 to Oct 2018 at the *C. maculata* site and from Oct 2017 to Jun 2021 at the *M. styphelioides* site.

The level survey data will be compared with the surface soil movement y_s determined by the soil profile and the soil moisture state affected by its regional climate (AS2870 2011). y_s can be estimated based on the soil design suction change profile and applying Eq. 1.

$$y_s = \frac{1}{100} \sum_{n=1}^N \left(I_{pt} \overline{\Delta u h} \right)_n \quad (1)$$

where N is the number of soil layers within the depth of design suction change H_s ; I_{pt} is the soil instability index estimated by a shrinkage index I_{ps} and a correction factor α . Δu is the mean suction change in the soil layer, and h is the depth of the soil layer.

The tree-induced extra surface soil movement y_t is determined using Eq. 2 by assuming the soil is fully cracked over the soil profile.

$$y_t = \left[1 - \left(\frac{\frac{D_i}{HT} - 0.5}{\frac{D_i}{HT} - 0.5} \right) \right] y_{tmax} \quad (2)$$

where y_{tmax} is the tree-induced maximum surface soil movement calculated following Eq. 1. D_i and D_j are the distance from the tree to the building and

the tree's influence distance, respectively. HT is the height of the tree.

Soil moisture

The Campbell 503DR Neutron Moisture Meter (NMM) has been widely used to measure soil water content due to its broad range of measurement, ease of use and capability to measure at greater depths (Li et al. 2003a, b). In this study, the NMM was employed to monitor volumetric soil moisture variations at various distances and depths from each tree. At each site, two 100 mm BHs were drilled to a depth of 3–4 m, which were cased with 50 mm diameter aluminium access tubes. The mixture of soils from the same BH and bentonite was used to backfill the gap between the boring wall and the access tube. The top of the BH was secured with a cast iron cover. For *C. maculata*, NMM measurements were taken at distances of 6.0 and 15.0 m away, and at depths ranging from 0.4 to 4.0 m. For *M. styphelioides*, measurements were taken at distances of 3.7 and 8.2 m away, and at depths ranging from 0.4 to 3.0 m.

The NMM includes a probe attached to a data logger via a cable. The probe comprises an encapsulated radioactive source (Americium-241: Beryllium) emitting high-energy neutrons and a detector. The fast neutrons released from the source collide with hydrogen in the soil and thermalize neutrons. The moderated neutrons counted by the detector are correlated with the level of water content in the soil. The duration of neutron counts can greatly affect the precision of NMM measurement, and it was approved that the use of 16 s counts can lead to a considerably precise measurement (Li et al. 2003b). The neutron count ratio (NCR) is the quotient of neutron readings in the soil divided by the background readings taken in the wax in the shield, and it has been commonly employed by users to avoid unacceptable drift of the electronics. The field calibration of NMM was conducted for each site. The volumetric water content was determined for silty clay samples obtained from various depths of BHs. The NMM readings for the same depth were undertaken shortly after, which allowed NCR to be calculated and subsequently correlated with volumetric water content measurements.

Sap flow meter

Sap flow, the water transport in the water-conducting xylem tissue of plants, has been widely used to estimate whole canopy transpiration for trees in the field site (Fernández et al. 2001; Nadezhdina et al. 2009). Among various types of heat pulse velocity based sap flow instruments, the Sap Flow Meter SFM1, which is based on the theory of heat ratio method, was approved to offer accurate sap flow measurements for a wide range of plant species (Burgess et al. 2001). In this study, one SFM1 was installed on the north side of each tree to monitor the tree soil water use. It was assumed both trees have a symmetrical cross-section. This study used SFM1 to monitor the soil water use of the two trees. The SFM1 include one heater needle and two temperature needles attached individually to the main body of the device. Two sensors are positioned at a distance of 7.5 and 22.5 mm from the tip of each temperature needle. After releasing a 20 J heat pulse from the heater, the thermistors measure the temperature differences in the sap transported upstream and downstream. Two 12 volts (18 A) external batteries in series placed in a stainless-steel case were connected to the SFM1 to enable continuous sap flow measurements. In order to maintain the uninterrupted operation of the SFM1, the site visit is scheduled every 21 days to replace the batteries used for charging SFM1 before they are depleted. The SFM1 was programmed to half-hourly logging intervals. The total soil water use of the tree was determined by multiplying the sap flow velocity recorded by SFM1 with the sapwood cross-sectional area.

Site investigation and laboratory test

In the field sites, BHs were drilled at distances of 6.0 and 15.0 m away from the *C. maculata*, and at distances of 3.7 and 8.2 m away from the *M. styphelioides* in October 2017 (Fig. 2). Soils obtained from BHs were used to develop soil profiles and perform soil laboratory tests, including soil water contents, total soil suctions, Atterberg limits, shrink-swells and soil water characteristic curve (SWCC).

The WP4 with a measurement range of 0–40 MPa and programmed with the chilled-mirror dewpoint technique was employed for the total soil suction measurement due to its ease to use and capability of providing fast and accurate measurements (Leong et al. 2003).

The potassium chloride solution was used to calibrate the instrument as recommended by the user manual.

The soil samples were crushed with a hammer following oven-drying at 105 °C for 24 h, which were then ground into fine particles using a mortar and pestle. Soil passing through the 425 µm sieve was used to conduct the Atterberg limits tests, including liquid limits, plastic limits and linear shrinkage according to AS1289 (2009a, b; 2008), respectively.

The shrink-swell test (AS1289 2003) contains a swelling test and a simplified core shrinkage test. The soil samples used to conduct shrink-swell tests were extracted from thin-walled 45 cm long and 5 cm diameter tubes pushed to two different depths at the tree's dripline (Fig. 2) using a hydraulic hammer. The 10 cm long soil core was prepared for the shrinkage test. A stainless-steel pin was pushed into the specimen at each end to provide a reference point that allowed the length change to be recorded. The mass and length of the specimen were measured three times a day during air-drying for two weeks and subsequently over-dried for 24 h. This allows the shrinkage strain ϵ_{sh} to be determined. For the swelling test, a 2 cm high and 4.5 cm diameter stainless-steel ring was pushed into the soil core and trimmed flat at both ends. Both top and bottom of the ring were attached with a porous stone and subsequently placed in a brass consolidation cell. An initial pressure of 5 kPa was applied to the specimen and then increased to 25 kPa for 30 min. Swell occurred following adding deionized water into the consolidation cell, and the induced displacements recorded by a data logger can be used to determine the swelling strain ϵ_{sw} . The shrink-swell index I_{ss} is calculated using Eq. 3. In this study, the shrink-swell tests were conducted at 0.8 and 1.7 m depth near the tree's dripline for each site, I_{ss} values other than the measured depth were estimated using the corresponding Plastic Index (PI) based on the I_{ss} – PI relationship recommended by Cameron (2017), although the correlation is likely to be conservative.

$$I_{ss} = \frac{\epsilon_{sh} + \frac{\epsilon_{sw}}{2.0}}{1.8} \quad (3)$$

Results

This section presents the results of soil tests and field measurements conducted at a 21-day interval for soil

movement, soil volumetric water content, and soil suction.

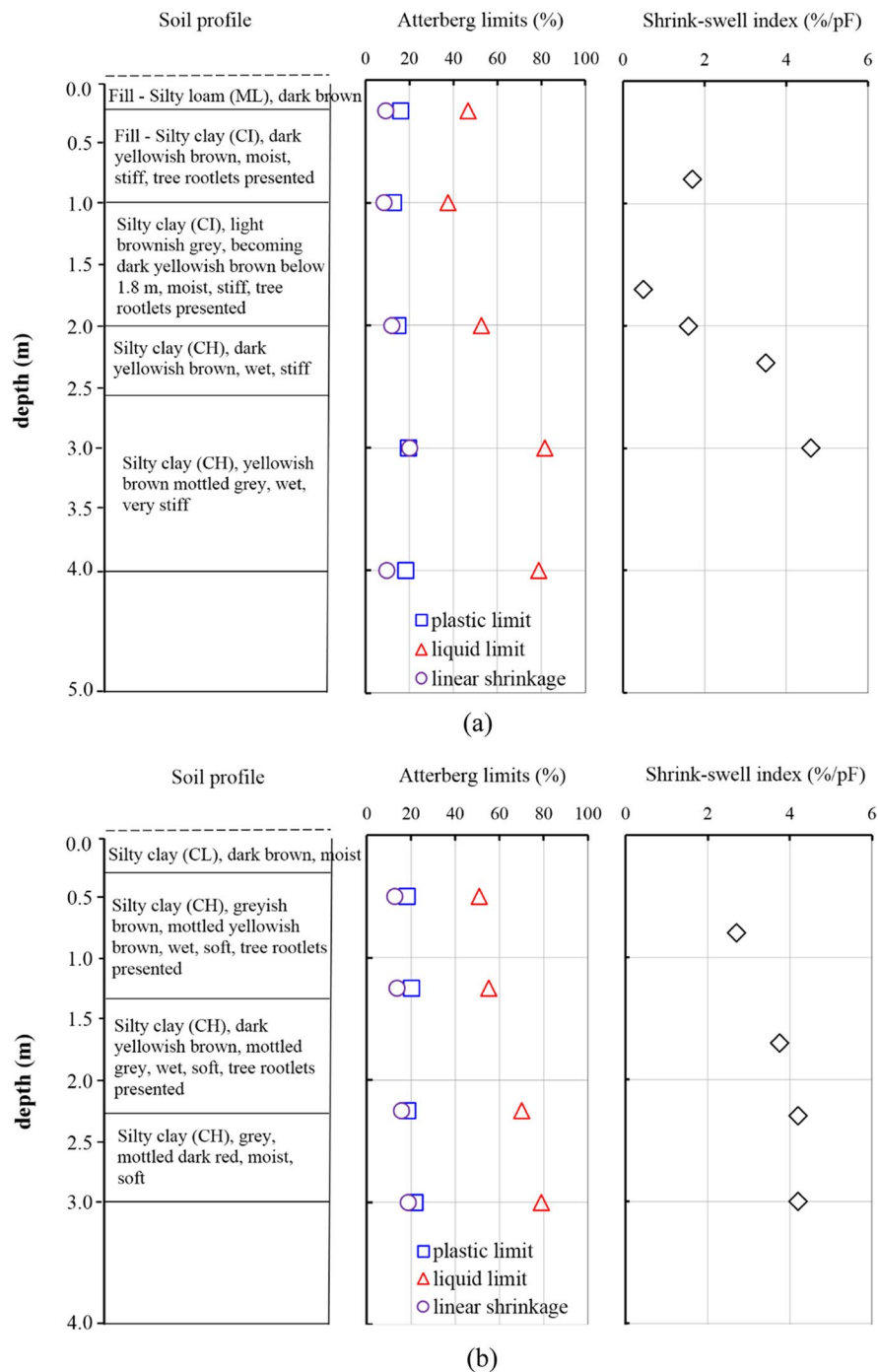
Soil test

The soil profile established for BH 1 at the *C. maculata* site is presented in Fig. 3a. The soil comprised 1 m of fill, including a layer of 0.1 m thick silty loam (ML), underlain by intermediate-plasticity silty clay, which became high-plasticity to 4 m deep (i.e. the full depth of investigation). At the *M. styphelioides* site, the soil comprised a 0.3 m thick layer of low-plasticity silty clay, which became high-plasticity to the full investigation depth of 3 m (Fig. 3b). The Atterberg limits test results for both sites revealed a relatively smaller variation of plastic limits and linear shrinkage over the depth of measurement. A marked increase in liquid limits occurred from 1.0 m (38%) to 3.0 m (82%) at the *C. maculata* site while a notable liquid limits rise by 28% was observed from 0.5 to 3.0 m at the *M. styphelioides* site. The shrink-swell indices I_{ss} at five different depths at the *C. maculata* site (Fig. 3a) show a significant increase in the I_{ss} from 0.5%/pF (low expansive) at 1.7 m to 4.6%/pF (high expansive) at 3.0 m. The I_{ss} at the *M. styphelioides* site (Fig. 3b) reveal that soil was highly expansive at the four measurement points. The surface soil movements y_s of 19 mm (Class S) and 35 mm (Class M) were determined for *C. maculata* and *M. styphelioides* site, respectively, using Eq. 1.

The SWCC drying curves established for the two study sites in Fig. 4 included 10 data points and were developed using the Fredlund SWC-150 for suction ranging between 10 kPa and 1500 kPa, and the Dew-point Potentiometer (WP4) was employed for suction exceeding 1500 kPa. The suction constraints of 0 kPa and 1,000,000 kPa were assumed. The equation introduced by Fredlund and Xing (1994) was used to best fit the measurement data.

The soil suction and water content profiles in February and October 2017 for BH 1 close to the *C. maculata* are presented in Fig. 5a. Each data point reported is the average of two sub-samples. The investigation was completed at 2.0 m deep in Feb 2017 due to push tube refusal. Soil suction was relatively low in October compared to soil sampled in the hotter month in February. The corresponding water content data revealed a similar trend of soil moisture condition with distinctly higher water content in October.

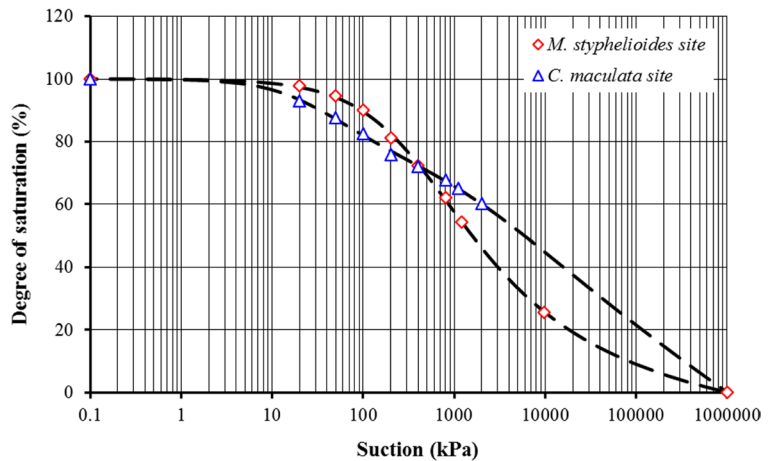
Fig. 3 Soil test results in close proximity to the experimental tree **a** *C. maculata* site **b** *M. styphelioides* site



In contrast, soil desiccation from 1.0 to 1.5 m during the tree growth season (i.e. October) was evident at the *M. styphelioides* site (Fig. 6a), and this finding was supported by the corresponding water content data. It is derived from soil suction and water content

data for 0–2 m in February and October at the *C. maculata* site that a change in the suction of 100 kPa would represent a change in water content of approximately 1%. Figure 5b presents the total soil suction and water content profiles for BH 2 in February and

Fig. 4 The SWCC drying curves developed for the two study sites



October. In contrast to soil obtained in October, soil suction ranged from 760 kPa to 1070 kPa in February, which was, on average, 28% higher over the full depth of measurement. It is noticed that soil suction remained constant below 2.5 m deep in both months, and the 1000 kPa could be taken as the wilting point suction u_{wp} for the site. A same u_{wp} value of 1000 kPa was obtained at the *M. styphelioides* site (Fig. 6a). As presented in Fig. 6a, when soil suction and water content data in February and October are compared, it is calculated that a 2% change in water content equates to a 100 kPa change in suction.

Ground and sub-ground soil movement

Figure 7a shows the level survey results in the vicinity of the *C. maculata* over 13 months. Compared to the soil further away from the tree, the soil closest to the dripline (i.e. surface pad 1, D_i : $HT=0.5$) experienced more significant shrinkage settlement in summer. At a distance of 7.3 m (D_i : $HT=0.5$) from the tree, a small amount of soil settlement of 4 mm was found at 0.5 m depth. A continuous upward soil movement was observed at 1.0 m depth from Dec 2017 to May 2018, with a maximum heave of 29 mm occurring at a distance of 11 m from the tree. This movement is 34% higher than the calculated y_s of 19 mm. The considerable heave at 1.0 m depth may be considered as the consequence of rainwater ingress due to the PVC locking cap being damaged by a lawnmower. A relatively smaller movement was observed from winter to early spring for both surface and sub-surface soil.

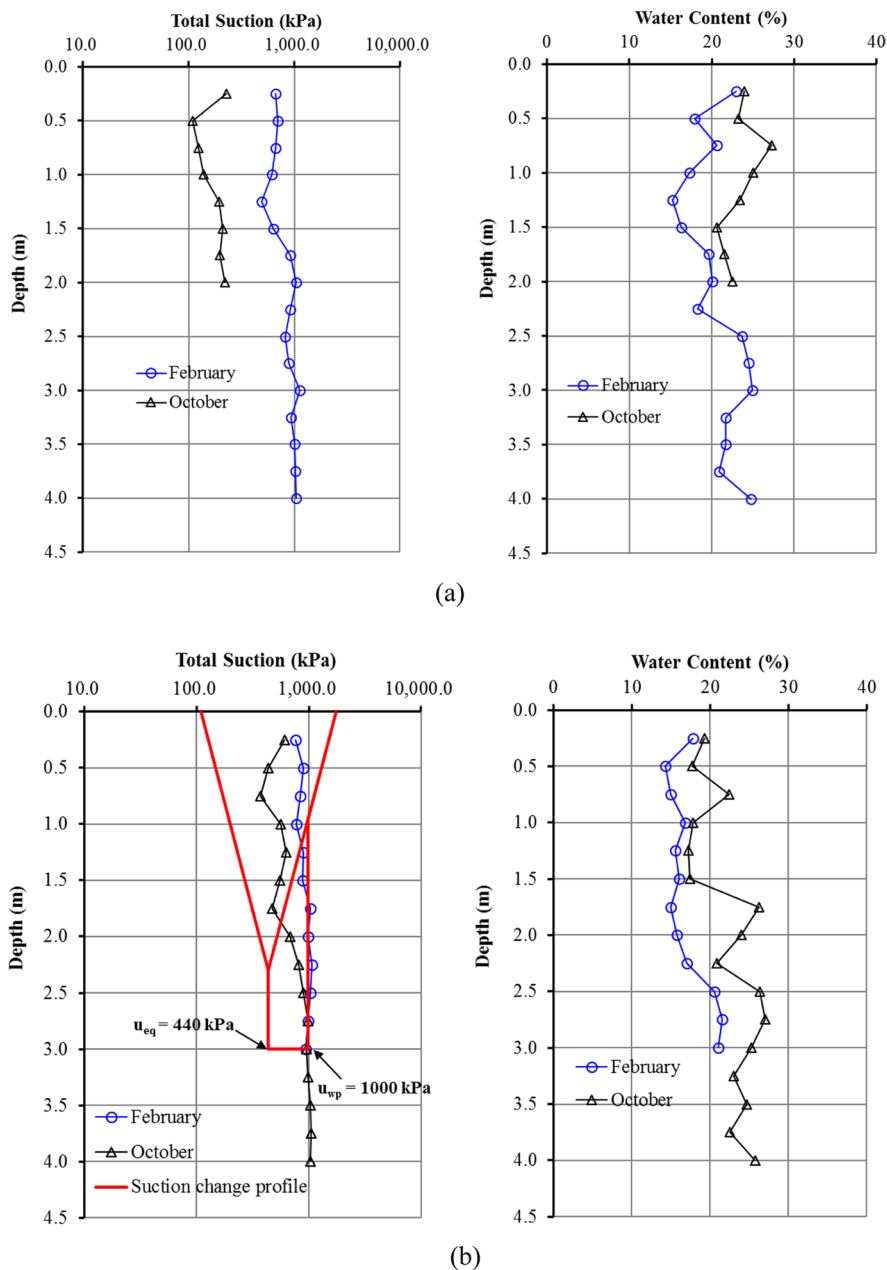
Figure 7b presents the variations in soil movement beneath the pavement, showing soil experienced a similar variation trend over 13 months. It is noted that Pin (3) experienced a small amount of settlement while the other four pins moved up on 10th Jan 2018. The Pin (5) showed the largest shrinkage settlement of 21 mm (D_i : $HT=0.7$) during the level survey conducted in March 2018, indicating localized shrinkage settlement likely caused by tree root drying.

Figure 8 presents the level survey data in the vicinity of the *M. styphelioides* for 45 months. Generally, soil experienced more heave than settlement over the study period, although both surface and sub-surface soil have exhibited a similar variation trend. The surface soil at a distance of 4.0 m from the tree (i.e. surface pad (1), D_i : $HT=0.5$) experienced the greatest shrinkage settlement of 9 mm compared to the soil located farthest from the tree. This trend is similar to the *C. maculata* tree site, likely due to the drying effect of high-density tree roots at the dripline. A significant heave was observed for all surface pads from Jan 2018 to May 2018, and from Nov 2018 to Mar 2019, with a maximum movement of 20.0 mm occurring at a distance of 8.0 m from the tree trunk. A marked downward movement, on average, occurred from 16 mm in May 2019 to -6 mm in Sep 2019 during the 2nd season cycle. For all the monitoring points, fewer soil movements occurred during the 4th season cycle.

Volumetric soil water content

Soil volumetric water content at various depths at distances of 6 m (P1) and 15 m (P2) away from the

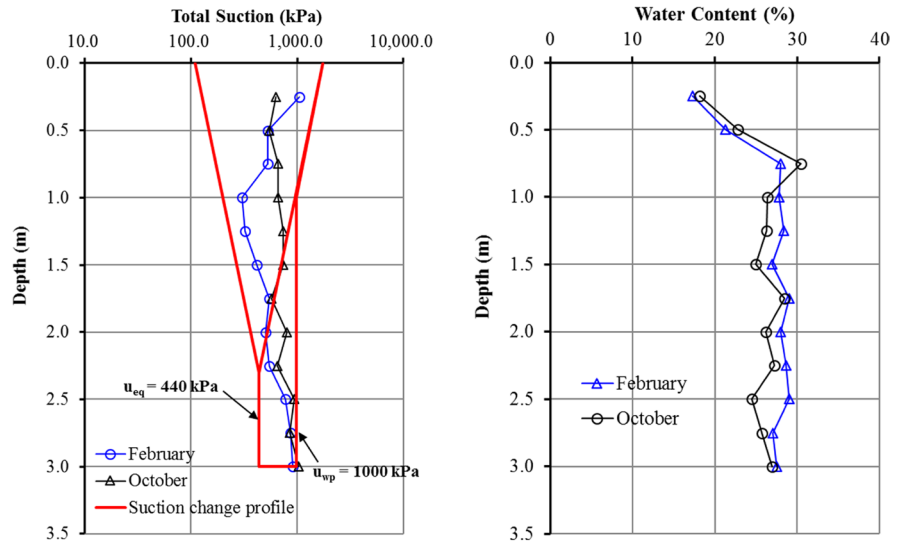
Fig. 5 Total soil suction and water content profiles close to the *C. maculata*
a BH 1 **b** BH 2



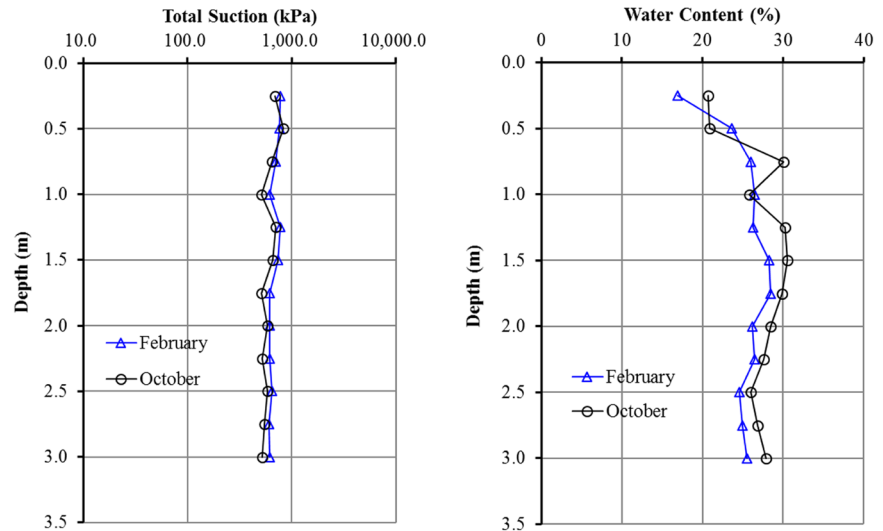
C. maculata over 13 months is presented in Fig. 9a. Soil water content near the dripline (i.e. P1) varies significantly from 9 to 32% within the top 1.1 m. The variation became smaller between 1.1 and 2.7 m and experienced little change below 2.7 m to the full measuring depth of 3.9 m. Volumetric soil water content profiles for P1 at the *M. stypelioides* site (Fig. 9b) show approximately 15% variation in volumetric water content within the top 2.1 m,

which lessened below this depth. An envelope was established using the maximal and minimal measurements at every depth across the full depth of measurement over the study period. The lowest soil water content ranging from 9 to 24% was observed between 0.4 and 2.1 m at the *C. maculata* site, with the noticeable tree-induced soil desiccation occurring at 1.1 m depth (Fig. 9a). In contrast, soil drying close to the dripline of the *M. stypelioides*

Fig. 6 Total soil suction and water content profiles close to the *M. styphelioides*
a BH 1 **b** BH 2



(a)



(b)

was evident between 0.6 and 2.2 m deep, with the lowest water content, on average, of 21% (Fig. 9b). For both sites, water content variations for P2 were substantially less when compared to water content changes at the same depth for P1.

Total soil suction

Three in-situ soil hygrometers were installed at 0.4 m, 1.4 m and 2.3 m depth in the pre-drilled borehole located 6.7 m away from the *C. maculata*.

Figure 10a shows the soil suction profiles established from measurements taken between Oct 2017 and Oct 2018. A significant variation in soil suction ranging from 10 kPa to 1390 kPa was observed at 0.4 m deep, which lessened below this depth until 1.4 m. This observation is confirmed by the soil volumetric water contents profile in Fig. 9a, which shows that the soil near the ground surface has experienced considerable variations in water content. The same trend was observed at the *M. styphelioides* site, with substantial variation in soil

Fig. 7 Soil movements at different distances from the *C. maculata* over 13 months **a** ground and sub-ground movements on the west side of the tree **b** ground movements on the south side of the tree

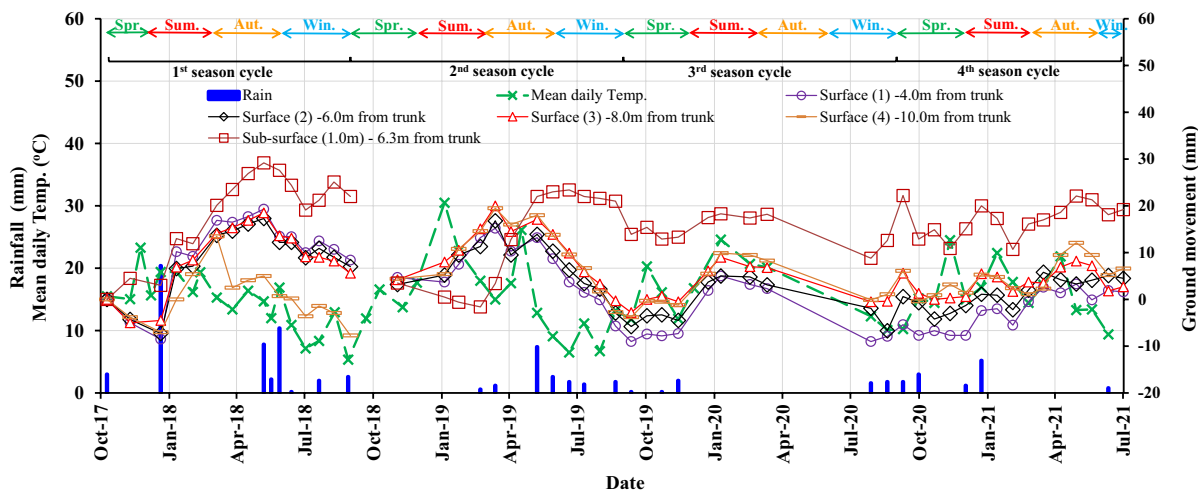
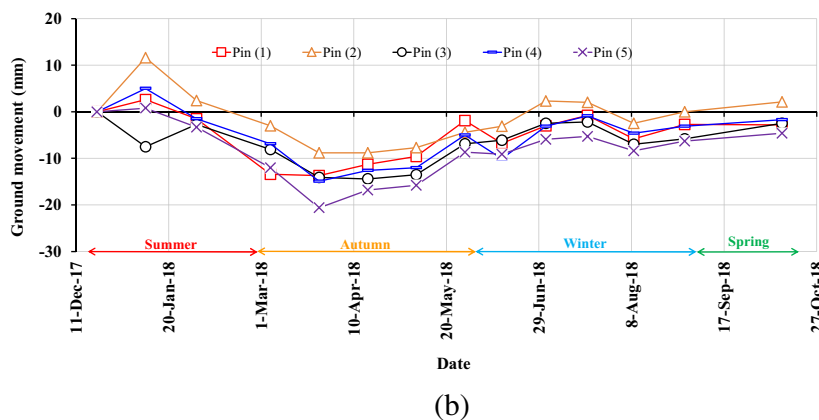
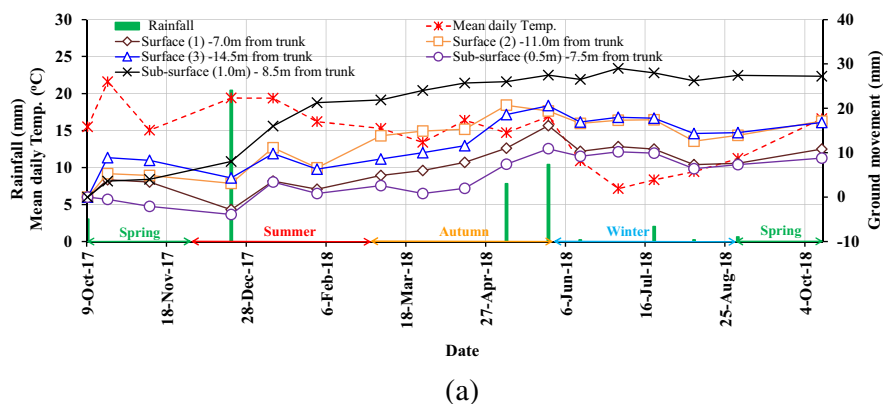
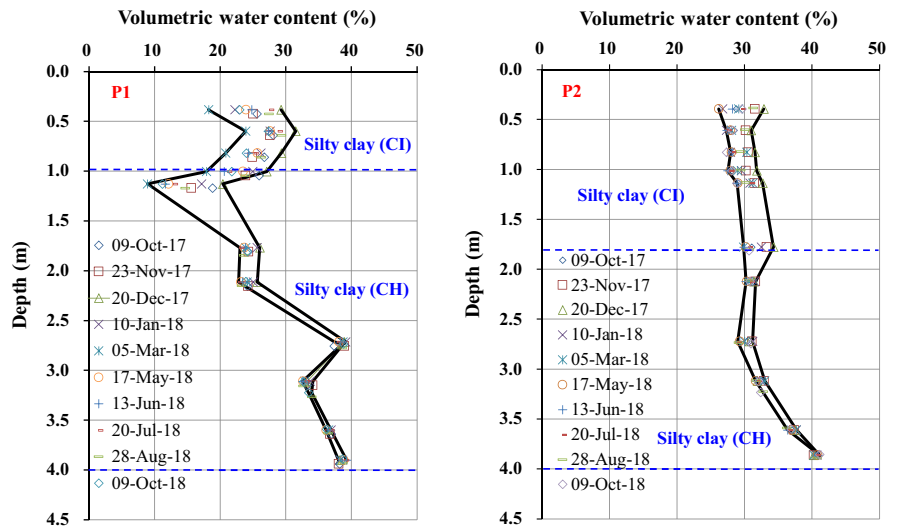


Fig. 8 Surface and subsurface soil movement close to the *M. styphelioides* over 45 months

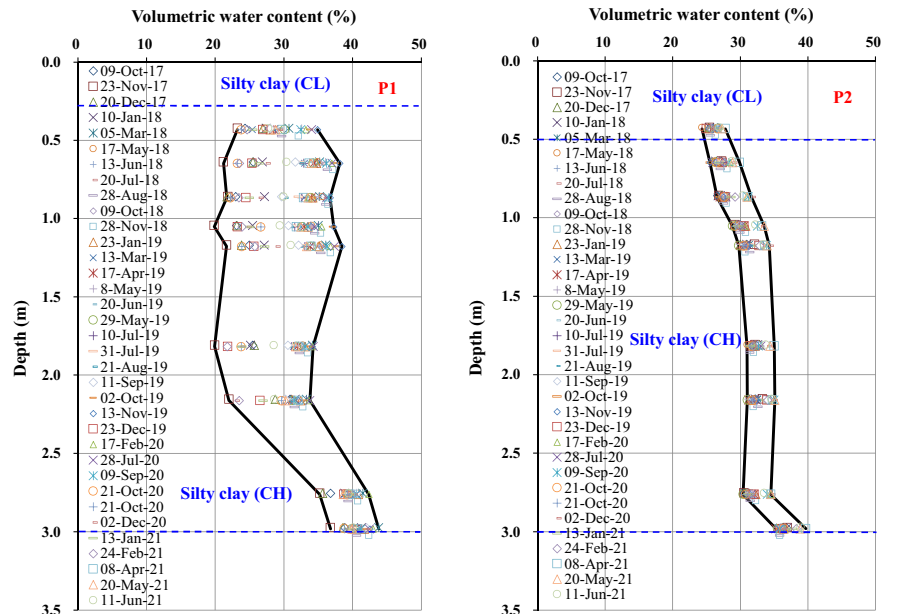
suction ranging from 10 kPa to 2240 kPa occurring at 0.4 m deep. The established upper envelope for the two sites reveals a wilting point suction u_{wp} of

1000 kPa, which is consistent with the estimated value in Figs. 5b and 6a. The soil at the *M. styphelioides* site experienced a suction change of 330 kPa

Fig. 9 Volumetric water content measurement results close to the sampled tree **a** *C. maculata* site **b** *M. styphelioides* site



(a)



(b)

between the dry limit (110 kPa) and the inferred u_{eq} (440 kPa) at 2.5 m deep (Fig. 10b), indicating the climate-induced suction change occurs deeper than the depth of 2.3 m provided by the Standard.

Tree soil water use

The daily sap flow rate logged by SFM1 on a 30 minus interval for the two trees over 28 days in

Feb 2018 is depicted in Fig. 11. The daily sap flow rate on the north side of both trees revealed a bell-shaped curve, with the sap flow peaking in the early afternoon and closer to zero flow at midnight following a gradual descent. A noticeable night-time sap flow was observed for both trees on the 24th of February, contributing 23% and 17% to the total daily amount. The slowest sap flow was found on the same day for the two trees, most likely due

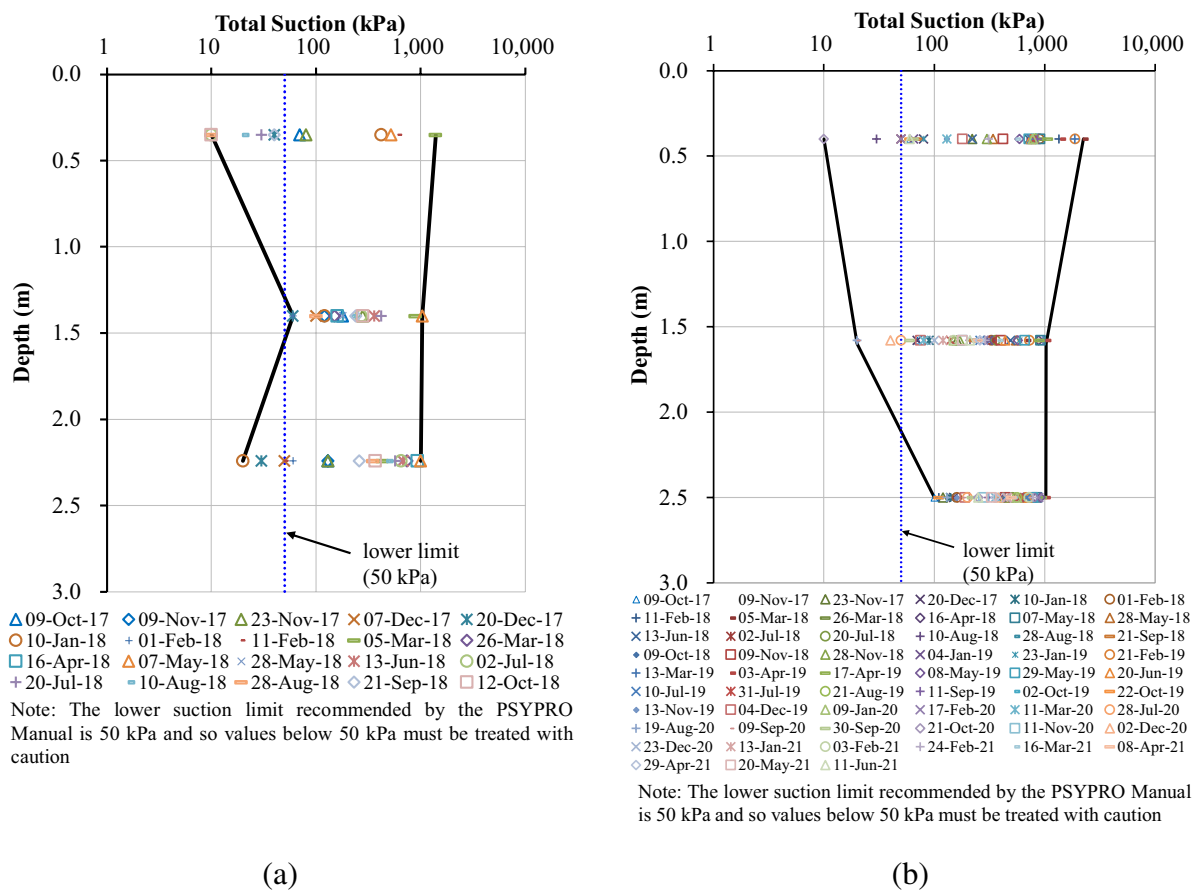
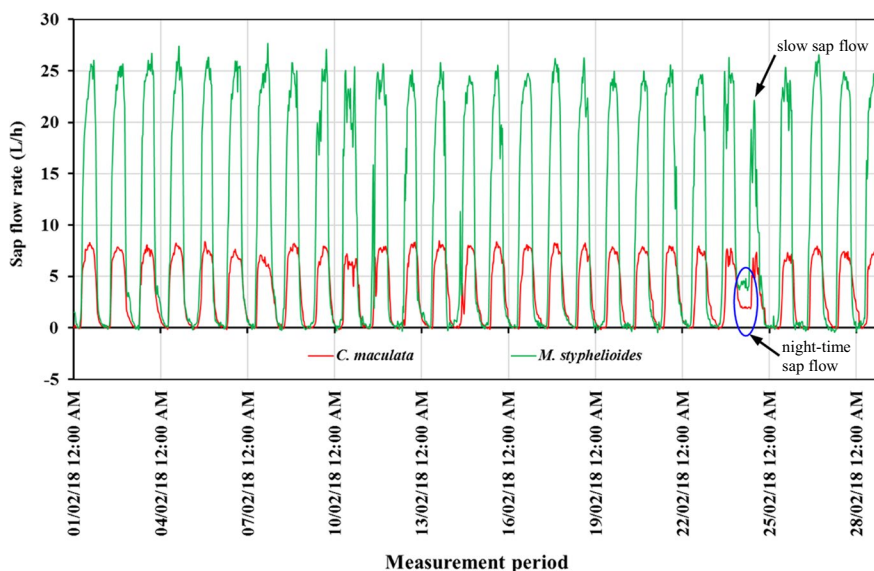


Fig. 10 Soil suction measurement results close to the sampled tree **a** *C. maculata* site **b** *M. styphelioides* site

Fig. 11 Comparison of daily sap flow rate for the two tree species over 28 days



to the lowest daily solar radiation of 3.2 MJ m^{-2} , which is 84% lower than the monthly mean.

The monthly sap flow volume variation pattern for *C. maculata* and *M. styphelioides* from Sep 2017 to Dec 2018 is presented in Fig. 12. A similar variation trend was observed for the two trees, with a significant sap volume rise from spring until mid-summer, followed by a gradual decrease through autumn and early winter. It should be noted that construction work was carried out close to the *C. maculata* in Nov 2018, leading to a marked reduction in the amount of water uptake by the tree. The monthly sap flow volume for both trees showed good agreement with two weather variables, monthly average temperature and solar radiation, as shown in Fig. 12.

Figure 13 shows a comparison of the monthly sap volume for the two trees in 2017 and 2018. The results indicate that the *C. maculata* extracted 10–57% more water from September to December 2017 than during the same period in 2018. The monthly transpiration of the *M. styphelioides* in 2017, on average, was 6% higher than that in 2018, with a marked water use reduction of 865 L occurring in September.

Response of soil characteristics to tree water uptake

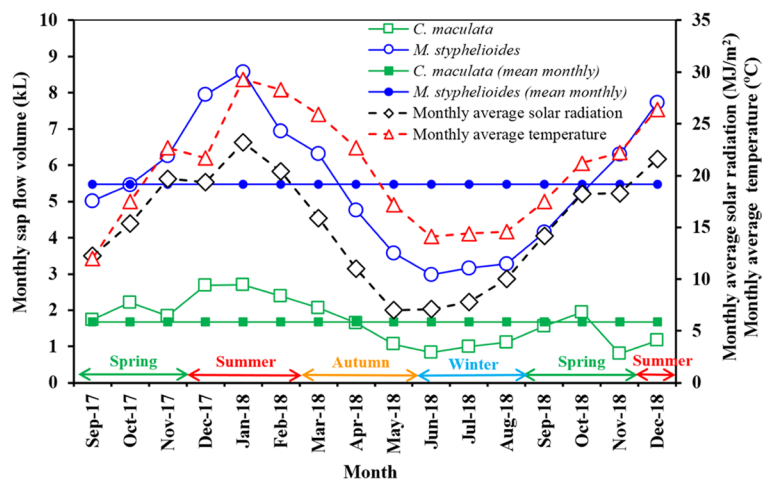
To investigate the causality and intercorrelation among ground movement, soil water content, soil suction and tree soil water use, the field measurement data for these variables from May 2019 to September 2019 close to the dripline of the *M. styphelioides* tree site was assessed. The chosen period revealed a

continuous soil settlement caused by the effect of tree root drying, which was not observed during the study period for the *C. maculata* site. The patterns for these variables are presented in Fig. 14. The correlation between ground movement, soil water content, soil suction and soil water use of the *M. styphelioides* is shown in Fig. 15.

Discussion

The design soil suction change profiles caused by local climate and tree-induced additional suction change were compared against the measurement-based suction profiles for the *C. maculata* site (Fig. 5b). The value of 440 kPa was determined for the deep equilibrium suction u_{eq} , based on the inferred u_{wp} and design value of Δu_{base} (i.e. 0.35 pF) given by the Standard. This value is much smaller than the u_{eq} of 980 kPa inferred for a 9 m high gum tree site, but similar to the value of 420 kPa reported for a site with a row of gum trees in South Australia (Cameron and Beal 2011). Sun and Li (2023a) estimated a u_{eq} of 610 kPa for a *C. maculata* tree site located 6 km away from the experimental site in this study. Li and Guo (2017) established soil suction profiles near a 15 m high Eucalypt at Williamstown, Melbourne, and found a u_{eq} value of approximately 1210 kPa for that site. The differences in u_{eq} values are likely due to variations in tree height, tree species and soil profile. The wilting point suction u_{wp} , was determined from the soil suction profiles for both sites, revealing that the root systems of the two tree

Fig. 12 Monthly variations in sap flow volume for the two tree species and monthly average temperature and solar radiation from Sep 2017 to Dec 2018



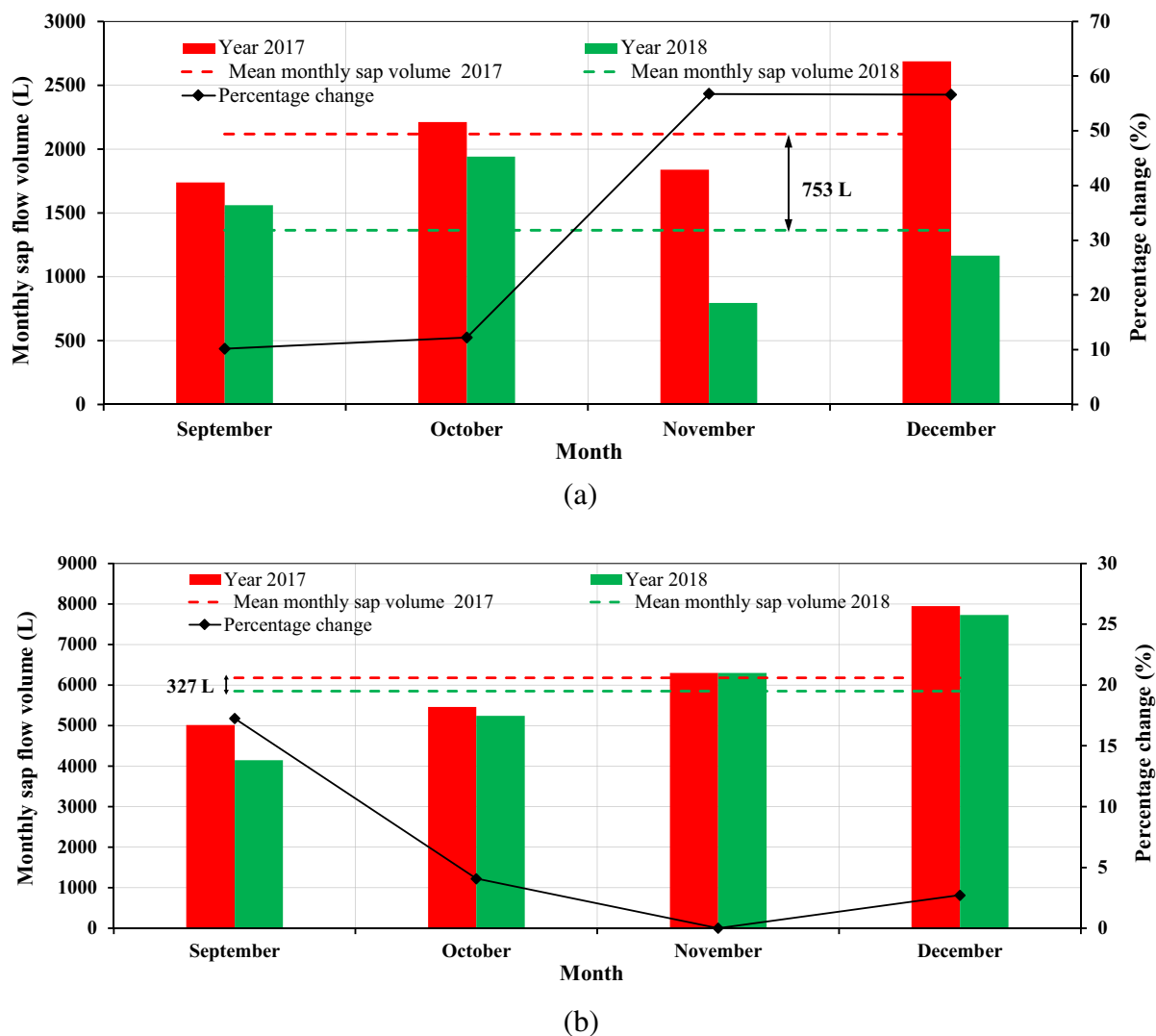


Fig. 13 Comparison of monthly sap flow volume of the sampled trees in two different years **a** *C. maculata* **b** *M. styphelioides*

species reached a point where they could no longer effectively extract water from the soil once the total soil suction exceeded the threshold of 1000 kPa. This finding is in concordance with the observations of Sun and Li (2023b), who reported a comparable u_{wp} of 4.04 pF (1,070 kPa) in proximity to a cluster of *C. maculata*. Furthermore, analogous research conducted by Cameron and Beal (2011) disclosed a u_{wp} value of 3.98 pF (930 kPa) at the outermost periphery of a row of eucalyptus trees.

Figures 5b and 6a suggest that soil suction change above 1 m depth was caused by climate variations and the effect of tree root drying was responsible for

the suction change from 1 to 3 m deep. Sun and Li (2023a) showed similar findings from the soil suction profile that the climate condition caused the variations in soil suction up to a depth of 0.7 m near a *C. maculata*; changes below this depth to 3 m were due to the drying effect of the tree roots. The established u_{wp} for both sites infers that soil shrinkage settlement has already happened prior to the study period (Sun et al. 2021).

The measured tree influential distance-to-tree height ratio of 0.7 was determined for the *C. maculata* site, which is significantly higher than the ratio of 0.4 observed for a *C. ficifolia* located in a north

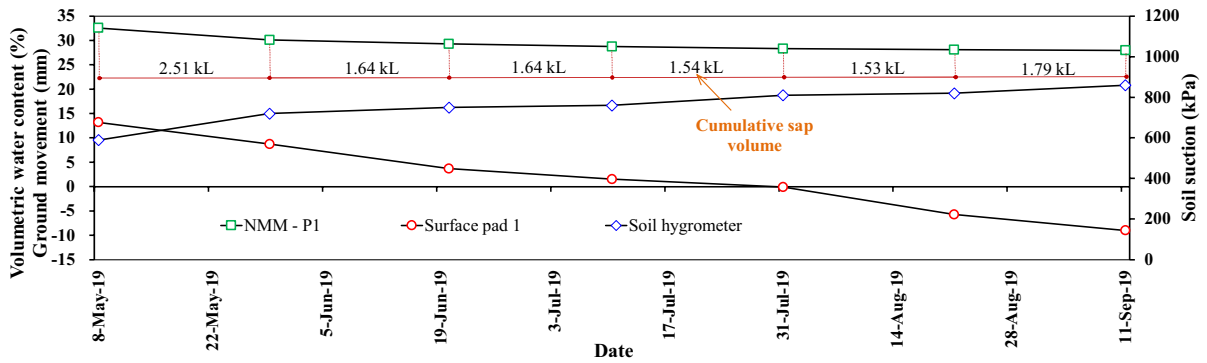


Fig. 14 Patterns of ground movement, soil water content, soil suction and tree soil water use from May 2019 to September 2019 for the *M. styphelioides* site

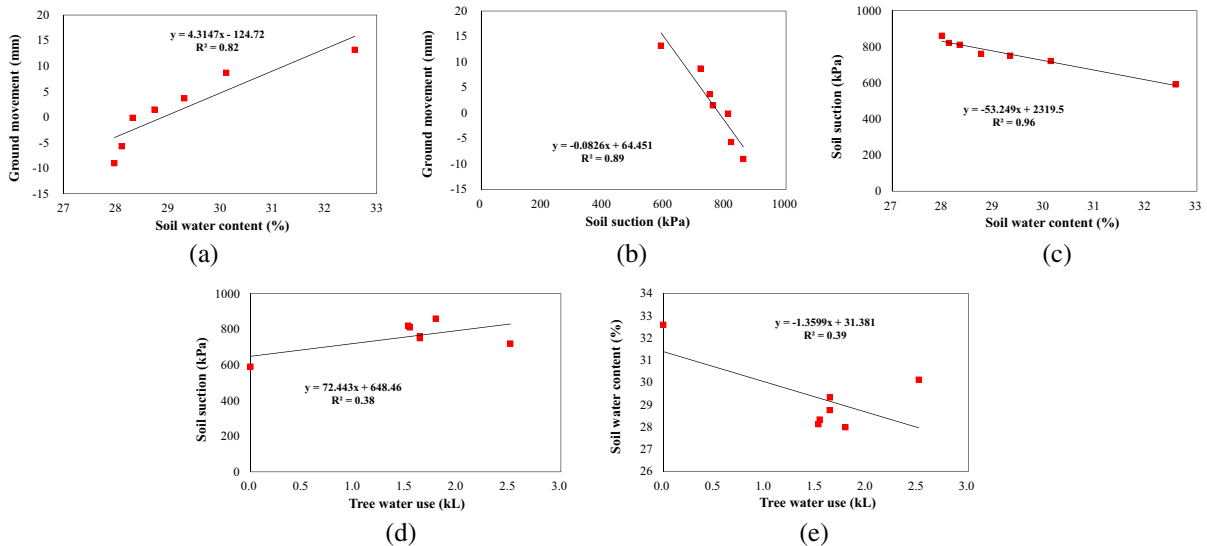


Fig. 15 Linear correlation between ground movement, soil water content, soil suction and tree soil water use of the *M. styphelioides*

suburb of Melbourne (Li et al. 2014). The lower influence exerted by the tree is likely attributed to its young age of only four years. The noticeable soil shrinkage settlement close to the dripline of *C. maculata* (D_i : $HT=0.5$) during summer is likely due to the higher density of tree roots at the dripline, resulting in a greater impact of tree root drying. The continuous settlement for almost all survey pins from January to March 2018 (Fig. 7b) may be explained by the increased soil water use of the tree during hotter periods (Li et al. 2014; Sun et al. 2022a, b). The soil on the south side of the tree exhibited greater movements compared to the west side, albeit with relatively small

changes from winter to early spring. This observation suggests that the roots have extended more towards the south side of the tree, likely due to higher soil water availability beneath the footpath than in the open ground on the west side. The influential distance (D_i : $HT=0.5$) of the *M. styphelioides* falls within the conservative threshold suggested by the Standard. The effect of daily rainfall and mean daily temperature on soil movements was assessed. From early February 2017 to early May 2018 (Fig. 7a), a continuous soil heave was observed at all measurement points at the *C. maculata* site, occurring a month after an intense rainfall event in late December. The

delayed upward soil movement could be attributed to the low permeability of clays (Sun and Li 2023a).

Soil volumetric water content profiles (Fig. 9a) established at the *C. maculata* site reveal a noticeable tree-induced soil desiccation at 1.1 m depth. This is consistent with the soil suction change profile established in Fig. 5b, suggesting the tree root drying effect commenced from 1 m deep. In contrast, the tree root drying effect between 0.6 and 2.2 m depth is evident close to the dripline of the *M. styphelioides* (Fig. 9b), as water content varied from 20 to 22% over these depths, significantly lower than soil ranging from 26 to 31% located 8.2 m away from the tree. Guswa (2008) demonstrated that climate and water availability exert primary control over the depth of root system. In ecosystems constrained by water availability, increased moisture levels resulting from climatic wetness lead to the development of deeper root systems. Notably, alterations in the duration of precipitation events have a more significant impact on root depth within such water-limited ecosystems compared to changes in the frequency of rainfall.

Quantifying the radial distance and depth propagated by soil moisture depletion from tree roots is crucial for predicting localized hydrologic impacts of urban trees. On a localized scale, determining the zone of soil desiccation close to urban trees allows the assessment of potential risks to surrounding infrastructure due to seasonal shrink-swell processes. On broader spatial scales, constraining the influences of lateral root spread and root depth through field evidence informs the parameterization and validation of hydrologic models simulating coupled tree-soil water dynamics at the landscape level (Fan et al. 2017).

The monthly soil water use by the *M. styphelioides* ranged from 3.0 kL to 8.6 kL, with the maximum and minimum sap volumes occurring in January and June, respectively. The variation trend of monthly sap flow volume is consistent with the soil water use pattern observed in four *M. styphelioides*, as reported by Sun et al. (2022a). The highest transpiration rate of 2.7 kL for the *C. maculata* also occurred in January, 66% lower than the water used by the *M. styphelioides*. Over the monitoring period, the *M. styphelioides* had transpired, on average, 5.5 kL of water per month, 69% higher than the mean monthly soil water used by the *C. maculata*. The differences in soil profiles between the two sites were a major factor contributing to the significant discrepancies in

tree soil water use (Carminati et al. 2016). Based on the calculated y_s , the *M. styphelioides* site was classified as moderately reactive while the *C. maculata* site was classified as slightly reactive. Highly reactive silty clays with I_{ss} ranging from 2.7%/pF to 4.2%/pF were distributed between 0.8 and 2.3 m at the *M. styphelioides* site. In comparison, the clay soil at the *C. maculata* site is less reactive, with the I_{ss} ranging from 0.5%/pF to 2.3%/pF over the same depth range (Fig. 3). The volumetric water content profiles (Fig. 9) close to the dripline also confirm that soil water content over these depths at the *M. styphelioides* site was, on average, 29% higher than that at the *C. maculata* site, providing sufficient water for tree roots to access. The SWCC drying curves developed for the two sites suggest that soil at *M. styphelioides* site is capable of retaining more water when subjected to suction below 400 kPa. It was found that 64% of the in-situ suction measurement data are smaller than this value. It is worth noting that the tree characteristics, such as water-conducting sapwood area, leaf and canopy size, and solar radiation interception, can significantly influence tree soil water use (Li and Guo 2017; Francescantonio et al. 2018; Sun et al. 2022a) and may contribute to the differences observed between the two sites. However, the discussion of these impacts is beyond the scope of this study. In November and December 2018, the *C. maculata* had transpired 1.8 kL and 2.7 kL of water, respectively, which is more than twice the amount used in the same month of the previous year. This increase in soil water use may explain the shrinkage settlement observed at various distances on the west side of the tree between October and December 2017, which resulted from a reduction in mean water content by 3% from 0.4 to 3.9 m depth (NP1). The mean monthly soil water use from September to December 2018 for the *C. maculata* has decreased by 753 L compared to sap flow volume for the same period in 2017. This is probably attributed to the reduced rainfall amount of 13.5% over the study period in 2018 (BOM 2022). The water uptake by the *M. styphelioides* was not influenced by the decline of rainfall in 2018, and it had used the same amount of water in November for two consecutive years. Quantifying the water demands of these popular native tree species within urban environments can help mitigate infrastructure risks, contribute significantly to advancing

sustainable design principles, and enable better management of urban forests.

The data analysis presented in Fig. 15a suggests that there is a strong positive linear relationship (R^2 of 0.82) between ground movement and soil water content, as both exhibited a very similar variation trend during the monitoring period. In contrast, there is a negative correlation between ground movement and soil suction, as an increase in soil suction leads to shrinkage settlement of the soil. Figure 15b shows that soil suction, as an independent variable, explains 89% variation in ground movement. As independent variables to ground movement, both soil water content and soil suction are intercorrelated (Li et al. 2014; Cameron and Beal 2011; Sun et al. 2021). A very strong linear correlation was demonstrated for these two variables, with soil water content responsible for 96% variation in soil suction (Fig. 15c). This trend was confirmed by the SWCC drying curve (Fig. 4), showing a reasonable linear correlation for suction ranging from 500 kPa to 900 kPa. Figure 15d-e reveals a poor correlation between soil water content, soil suction and tree soil water use. This is because other than water extraction by tree roots, climate factors such as air temperature, precipitation and evapotranspiration could also influence soil water dynamics to an inferred depth of 1 m (Sun and Li 2023a). Besides, the amount of water used by the tree cannot entirely explain variations in soil suction and water content since tree root absorbs water not only at the dripline where soil water dynamics were measured but also at various distances and orientations from the tree. Overall, the correlation of these measured variables suggests that tree root water uptake of 10.64 kL from May 2019 to September 2019 partially contributes to a decline in soil water content from 33 to 28% and a rise in soil suction from 590 kPa to 860 kPa, resulting in a continuous soil settlement of 22 mm.

Conclusions

The drying effects of root systems from two popular Australian native tree species on soil water dynamics and movement were assessed for up to 45 months in two well-established sites located in Melbourne,

Australia. This study finds that the drying influence of root system of *C. maculata* extended to a radial distance of 10 m (D_i : $HT=0.7$) and a depth of 1.1 m, whereas for the *M. styphelioides* site, the drying influence reached a distance of 4 m (D_i : $HT=0.5$) and a depth of 2.2 m. Knowledge of the root-affected zone by those tree species enables evaluating threats to proximate infrastructure integrity arising from moisture variation-driven shrink-swell behaviors of expansive soils across wetting and drying cycles. The methodological framework developed in this study has the potential to be applied for investigating the soil desiccation induced by other tree species across diverse climate zones, along with its impacts on slope stability, buildings, roads, and other infrastructure.

Accurately assessing the water requirements of these urban trees can aid in mitigating potential infrastructure vulnerabilities. The long-term sap flow data for the two native tree species is scarce but essential as urban tree coverage expands. The high-quality tree soil water use information could be used to assess the suitability of tree species for applications like phytoremediation and revegetation by matching site conditions with plant water requirements.

Long-term, high-quality field measurement data, similar to what has been reported in this paper, can serve local governments in assessing tree water consumption and aiding in the selection of street tree species. This, in turn, supports the development of efficient and sustainable urban tree-planting management plans. Researchers can employ the tree soil water use and soil water dynamics datasets to calibrate numerical models of tree root water extraction and evaluate additional soil suction resulting from similar tree species with comparable characteristics across silty clay sites in temperate climates.

Acknowledgements The authors would like to extend their sincere appreciation for the financial and technical support provided by both the City of Knox and FMG Engineering.

Author contributions Conceptualization (XS and JL), methodology (XS), software (XS), investigation (XS and JL), validation (XS and JL), analysis (XS), resources (XS and JL), data curation (XS and JL), visualization (XS), writing (XS and JL), project administration (JL) and funding acquisition (JL). All authors approved the final version of the manuscript.

Funding Open Access funding enabled and organized by CAUL and its Member Institutions This work was supported

by the Australian Research Council through the ARC Linkage Grant LP16160100649.

Data availability The datasets generated during and/or analysed during the current study are available from the corresponding author on reasonable request.

Declarations

Conflict of interest The authors have no conflict of interest to declare.

Open Access This article is licensed under a Creative Commons Attribution 4.0 International License, which permits use, sharing, adaptation, distribution and reproduction in any medium or format, as long as you give appropriate credit to the original author(s) and the source, provide a link to the Creative Commons licence, and indicate if changes were made. The images or other third party material in this article are included in the article's Creative Commons licence, unless indicated otherwise in a credit line to the material. If material is not included in the article's Creative Commons licence and your intended use is not permitted by statutory regulation or exceeds the permitted use, you will need to obtain permission directly from the copyright holder. To view a copy of this licence, visit <http://creativecommons.org/licenses/by/4.0/>.

References

- AS 1289 (2008) Methods for testing soils for engineering purposes, Method 3.4.1, soil classification tests – determination of the Linear shrinkage of a soil (Standard Method). Standards Australia International Ltd, Sydney, Australia
- AS 1289 (2009a) Methods for testing soils for engineering purposes. Method 3.1.2, soil classification tests – determination of the Liquid of a soil– one point Casagrande Method (Subsidiary method). Standards Australia International Ltd, Sydney, Australia
- AS 1289 (2009b) Methods for testing soils for Engineering purposes, Method 3.2.1, soil classification tests – determination of the plastic limits of a soil (Standard Method). Standards Australia International Ltd, Sydney, Australia
- AS 2870 (2011) Residential slab and footings. Standards Australia International Ltd, Sydney, Australia
- AS1289 (2003) Methods for testing soils for Engineering Purposes, Method 7.1.1, determination of the Shrinkage Index of a soil; Shrink Swell Index. Standards Australia International Ltd, Sydney, Australia
- Biddle PG (1983) Patterns of soil drying and moisture deficit in the vicinity of trees on clay soils. *Geotechnique* 33(2):107–126
- BOM (Bureau of Meteorology) (2022) Climate Data Online. <http://www.bom.gov.au/climate/data/>. Accessed 11 May 2022
- Burgess SSO, Adams MA, Turner NC, Beverly CR, Ong CK, Khan AAH, Bleby TM (2001) An improved heat pulse method to measure low and reverse rates of sap flow in woody plants. *Tree Physiol* 21:589–598
- Cameron DA (2001) The extent of soil desiccation near trees in a semi-arid environment. *Geotech Geol Eng* 19:357–370
- Cameron DA (2017) Dealing with reactive clay soils through a national standard. *Aust Geomech J* 53(1):54–65
- Cameron DA, Beal NS (2011) Estimation of foundation movement and design of footing systems on reactive soils for the effects of trees. *Aust Geomech J* 46(3):97–113
- Carminati A, Zarebanadkouki M, Kroener E, Ahmed MA, Holz M (2016) Biophysical rhizosphere processes affecting root water uptake. *Ann Bot* 118:561–571
- Couvreur V, Ledder G, Manzoni S, Way DA, Muller EB, Russo SE (2018) Water transport through tall trees: a vertically explicit, analytical model of xylem hydraulic conductance in stems. *Plant Cell Environ* 41:1821–1839
- Dasgupta P, Dasa BS, Sen SK (2015) Soil water potential and recoverable water stress in drought tolerant and susceptible rice varieties. *Agric Water Manag* 152:110–118
- Dobson MC, Moffat AJ (1995) A re-evaluation of objections to tree planting on containment landfills. *Waste Manag Res* 13:579–600
- Fan Y, Míguez-Macho G, Jobbágy EG, Jackson RB, Otero-Casal C (2017) Hydrologic regulation of plant rooting depth. *Proc Natl Acad Sci USA* 114(40):10572–10577. <https://doi.org/10.1073/pnas.1712381114>
- Fernández JE, Palomo MJ, Díaz-Espejo A, Clothier BE, Green SR, Girón IF, Moreno F (2001) Heat-pulse measurements of sap flow in olives for automating irrigation: tests, root flow and diagnostics of water stress. *Agric Water Manag* 51(2):99–123
- Francescantonio DD, Villagra M, Goldstein G, Campanello PI (2018) Leaf phenology and water-use patterns of canopy trees in Northern Argentinean subtropical forests. *Tree Physiol* 38(12):1841–1854
- Fredlund DG, Xing A (1994) Equation for the soil-water characteristic curve. *Can Geotech J* 31(4):521–532
- Guswa AJ (2008) The influence of climate on root depth: a carbon cost-benefit analysis. *Water Resour Res* 44(2):W02427. <https://doi.org/10.1029/2007WR006384>
- Holland JE (1981) The design, performance and repair of Housing Foundations. Swinburne Institute of Technology, Melbourne, Australia
- Leong EC, Tripathy S, Rahardjo H (2003) Total suction measurement of unsaturated soils with a device using the chilled-mirror dew-point technique. *Geotechnique* 53(2):173–182
- Li J, Guo L (2017) Field investigation and numerical analysis of residential building damaged by expansive soil movement caused by tree root drying. *J Perform Constr Facil* 31(1):1–10
- Li J, Smith DW, Fityus SG (2003a) The Effect of a gap between the Access Tube and the soil during Neutron Probe measurements. *Aust J Soil Res* 41:151–164
- Li J, Smith DW, Fityus SG, Shen D (2003b) Numerical analysis of Neutron Moisture Probe measurements. *Int J Geomech* 3(12):11–20
- Li J, Sun X (2015) Evaluation of changes of the Thornthwaite Moisture Index in Victoria. *Aust Geomech J* 50(3):39–49
- Li J, Zhou Y, Guo L, Tokhi H (2014) The establishment of a field site for reactive soil and tree monitoring in Melbourne. *Aust Geomech J* 49(2):63–72

- Manoli G, Bonetti S, Domec JC, Putti M, Katul G, Marani M (2014) Tree root systems competing for soil moisture in a 3d soil–plant model. *Adv Water Resour* 66:32–42
- Nadezhdina N, Steppe K, De Pauw DJW, Bequet R, Cermak J, Ceulemans R (2009) Stem-mediated hydraulic redistribution in large roots on opposing sides of a Douglas-fir tree following localized irrigation. *New Phytol* 184(4):932–943
- Ng CWW, Wang ZJ, Ni JJ (2020) Effects of plant morphology on root–soil hydraulic interactions of *Schefflera heptaphylla*. *Can Geotech J* 58(5):666–681
- Silva M, Matheny AM, Pauwels VRN, Triadis D, Missik JE, Bohrer G, Daly E (2022) Tree hydrodynamic modelling of the soil–plant–atmosphere continuum using FETCH3. *Geosci Model Dev* 15:2619–2634
- Sun X, Li J (2023a) A parametric study of the effect of trees on residential footing design on expansive soils. *Geotech Geol Eng* 41(4):1–17. <https://doi.org/10.1007/s10706-023-02400-0>
- Sun X, Li J (2023b) Case study of ground subsidence caused by the drying effect of a group of Australian native eucalypts. *J Perform Constr Facil* 37(5):1–11. <https://doi.org/10.1061/JPCFEV.CFENG-4254>
- Sun X, Li J, Cameron DA, Moore G (2022a) Sap flow monitoring of two Australian native tree species in a suburban setting: implications for tree selection and management. *Plant Sci* 317. <https://doi.org/10.1016/j.plantsci.2022.111194>
- Sun X, Li J, Cameron DA, Moore G (2022b) On the use of sap flow measurements to assess the water requirements of three Australian native tree species. *Agron* 12(1):52. <https://doi.org/10.3390/agronomy12010052>
- Sun X, Li J, Cameron DA, Zhou AN (2021) Field monitoring and assessment of the impact of a large eucalypt on soil desiccation. *Acta Geotech* 17(3):1971–1984. <https://doi.org/10.1007/s11440-021-01308-4>
- Sun X, Li J, Zhou AN (2017) Assessment of the impact of climate change on expansive soil movements and site classification. *Aust Geomech J* 52(3):39–50
- Teodosio B, Pauwels VRN, Loheide SP, Daly E (2017) Relationship between root water uptake and soil respiration: a modelling perspective. *J Geophys Res Biogeosci* 122:1954–1968. <https://doi.org/10.1002/2017jg003831>
- Verma P, Yeates J, Daly E (2011) A stochastic model describing the impact of daily rainfall depth distribution on the soil water balance. *Adv Water Resour* 34:1039–1048

Publisher's Note Springer Nature remains neutral with regard to jurisdictional claims in published maps and institutional affiliations.